Journal of
Marine Science and Engineering

Article

Effect of Winding Steel Wire on the Collapse Pressure of Submarine Hose

Daifeng Wei [1], Chen An [1,*], Jixiang Zhang [1,2], Yixuan Huang [1] and Chenwang Gu [1]

1 College of Safety and Ocean Engineering, China University of Petroleum-Beijing, Beijing 102249, China
2 Centre for Marine Technology and Ocean Engineering (CENTEC), Instituto Superior Técnico, Universidade de Lisboa, 1049-001 Lisbon, Portugal
* Correspondence: anchen@cup.edu.cn

Abstract: The submarine hose plays a vital role in the single-point mooring system and is a necessary channel for medium transportation. Once crushed under the load of the seawater external pressure, it will cause oil and gas leakage and major safety accidents. It is a composite hose composed of a rubber layer, cord layer and steel helix wire, of which the steel helix wire plays an important part in bearing mechanical properties. In this work, python language was used to model the submarine hose parametrically, the finite element (FE) analysis software ABAQUS was utilized to analyze the ultimate bearing capacity of the hose under uniformly distributed external pressure loads and the influence of the initial ovality of the submarine hose, the diameter and pitch of the helix wire, the yield strength of the helix wire material on the ultimate bearing capacity of the submarine hose were studied. Through a large number of FE results, the ultimate bearing capacity of the hose was obtained by fitting the prediction formula.

Keywords: submarine hose; steel helix wire; collapse analysis; rebar

Citation: Wei, D.; An, C.; Zhang, J.; Huang, Y.; Gu, C. Effect of Winding Steel Wire on the Collapse Pressure of Submarine Hose. *J. Mar. Sci. Eng.* **2022**, *10*, 1365. https://doi.org/10.3390/jmse10101365

Academic Editor: Eva Loukogeorgaki

Received: 25 August 2022
Accepted: 21 September 2022
Published: 23 September 2022

1. Introduction

According to different mooring methods, commonly used offshore oil terminals are divided into multi-buoy mooring systems, fixed dock mooring systems, single-point mooring systems and fixed tower mooring systems. The catenary single-point mooring system (CALM) is the earliest type of single-point mooring system and is currently most widely used [1]. There are about 600 in practice around the world, mainly distributed in Southeast Asia and the Mediterranean coast of Europe. The main structures are buoys, mooring systems, mooring lines, floating hoses, submarine hoses, rotary joints, etc. [2].

One end of the submarine hose is connected to the flange on the Pipe Line End Manifold (PLEM), and the other end is connected to the rigid pipeline at the bottom of the buoy, as shown in Figure 1. The static form of the submarine hose is maintained by a float with certain buoyancy attached to the hose [3,4]. As shown in Figure 2, a submarine hose with larger diameter, lower bending stiffness and external pressure bearing capacity has undergone extensive application, which is a necessary channel for medium transportation and a significant part of CALM system design. Collapse damage will cause leakage, leading to monetary loss and environmental harm [5]. Hence, research into collapse bearing capacity for submarine hose is of considerable significance.

The submarine hose is composed of reinforcement fiber layers, rubber layers and steel helix wire, as shown in Figure 2. The inner rubber layer with H_2S corrosion resistance capacity was normally made from nitrile butadiene rubber (NBR) in the submarine hose. The second and fourth layers are wrapped with a good deal of cord fabric to form the reinforcement layer. The main function of the steel helix wire embedded in the middle rubber layer is to increase the mechanical properties of the hose, including resistance to internal and external pressure, tensile force and bending moment. The outer rubber layer of the submarine hose has protective and corrosion resistance properties. Those layers are bonded together and vulcanized in a uniform manner to withstand external loads in engineering application.

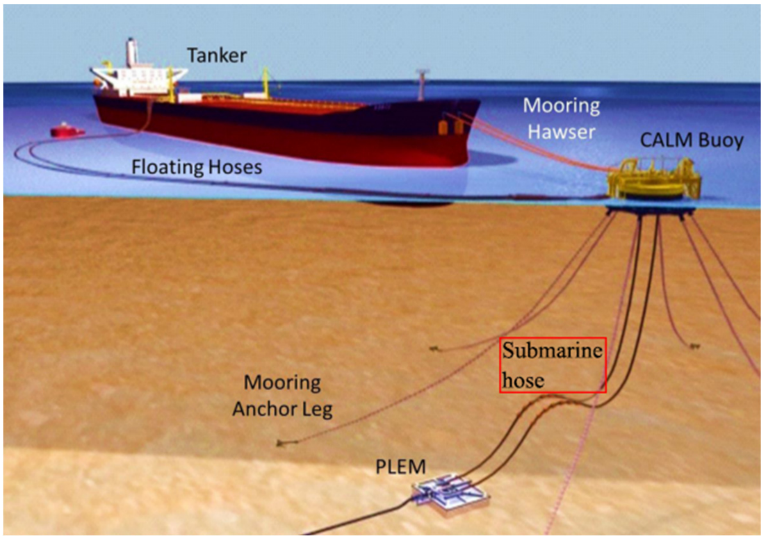

Figure 1. Schematic diagram of single point mooring system.

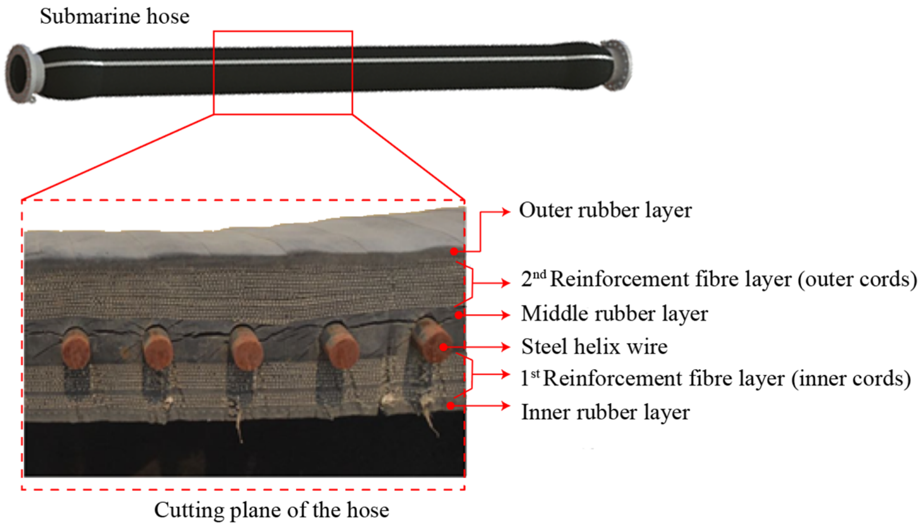

Figure 2. Submarine hose and the cross section.

At present, the technical specifications for the design, manufacture and testing of submarine hoses are mainly the specifications issued by the Oil Companies International Marine Forum (OCIMF) and the API standards [6,7].

The mechanical behavior of the floating hose was widely studied [8], yet there are few studies on submarine hoses. Gao et al. (2018) [9] and Tonatto et al. (2017) [10] analyzed the failure behavior of composite pipe under internal pressure load using ABAQUS software, respectively. Extended finite element method (XFEM) has recently been proposed to predict the failure of pipelines [11,12]. Based on nonlinear cable-like response to lift and Morison-type drag forces, Huang and Leonard (1990) [13] studied the lateral stability of the submarine hose under slowly changing current, which shows that for the actual hose, the most critical parameters are the ratio of section length to span, the axial stiffness of the hose, the hose size and the current speed. Ma et al. (2017) [14] analyzed the environmental load characteristics of submarine hoses, established a slender member model of submarine hoses considering the interaction of the internal fluid of the submarine hose and the external environmental load. The deformation of submarine hoses under different water currents and directions as well as the most vulnerable parts of submarine hoses were obtained, which has a vital reference value for the design of submarine hoses. Yang et al. (2018) [15] summarized the design and manufacturing requirements, some of working conditions, environmental loads and technical requirements of Chinese lantern-shaped submarine hoses were analyzed, and case study of dynamic response and fatigue analysis of submarine hoses was conducted. Wang et al. (2019) [16] conducted dynamic analysis on the Chinese lantern type and Lazy-S type submarine hoses, and studied the effects of wave height, flow angle, soil stiffness and hose hydrodynamic load on the structural behaviour of submarine hoses. Amaechi et al. (2019) [17] developed a coupled dynamic model including buoys and hoses, and carried out parameter studies to analyze the influence of the hose hydrodynamic load, flow angle, bending moment, effective tension and minimum bending radius on the structural behavior of the hose.

At present, the primary research on submarine hoses focuses on the cause discussion of engineering accidents and design methods, and the structural design of submarine hoses with resistance to external pressure has not formed a unified specification. The existing results adopt slender rod models for the mechanical response of submarine hoses, which are easily affected by the environment. The resistance ability to external pressure of submarine hoses has not been explored from the perspective of theoretical analysis and simulation analysis, and no specific model has been established. Subsequently, a study on the collapse of submarine hoses is of great significance to the structural design of submarine hoses.

In this paper, a finite element model combined with the nonlinear analysis method for the collapse analysis of the submarine hose with initial ovality is established and analyzed, considering the influence of the geometric parameters and material parameters of the helix wire on the collapse pressure of the submarine hose, based on the abundant results of finite element models, nonlinear least squares fitting is performed to obtain the prediction formula of the collapse pressure of submarine hoses.

2. Finite Element Model of Submarine Hose

Due to the complex structure of submarine hoses, the mechanical model is established under the following series of assumptions:

(1) Each layer structure of the submarine hose is an ideal cylindrical layer without manufacturing defects.

(2) The processing and manufacturing of the submarine hose body does not bring about pre-stress and strain.

(3) The layers of the submarine hose body, the reinforcing material and the base material are kept tightly bonded in the initial state and other various actual engineering conditions.

(4) The cross section at any position of the submarine hose body remains parallel after being subjected to external loads.

(5) Select the middle section of the submarine hose pipe body for finite element analysis and expect that the performance of the middle section can represent the entire pipe body.

Rubber, cords and steel helix wire are the main components of the composite hose. The embedded technology is used to simulate the interaction of each material, and the rebar element is used to simulate the mechanical behavior of the fiber cord. Wei et al. (2022) [18] and Gao et al. (2018) [9] use the embedded technology and the rebar element to simulate the mechanical behavior of the same type composite hose under the torsional load and the inner pressure, and uses a series of tests to verify the validity of the finite element model. At the same time, riks method is a effective technique for buckling and crushing analysis. An et al. (2014) [19], Bai et al. (2016, 2018) [20,21] and Yang et al. (2020) [22] used the riks method by the Abaqus software to study the buckling behavior of the composite pipes (sandwich pipe and SSRTP pipe) and verified them with experiments. For the validation of the finite element model, it is reliable to study buckling behavior of the composite hose under the external pressure through the embedded technology, rebar element and the riks method.

2.1. Simplification of the Hose Model

In this work, a certain type of submarine hose is carried out to study the collapse property of the hose under external pressure. The submarine hose dimensions are length of 10.7 m, inner diameter of 500 mm and both ends have steel flanges as connectors. In order to reduce the calculation amount of finite element analysis, the 3000 mm middle section of the pipe body was split to eliminate the influence of stress concentration according to Saint-Venant principle. Since the floating body ring and the outer protective layer had a negligible contribution to the mechanical properties of the structure, which can be ignored when building the model. The model structure from the inner to the outer is: inner rubber layer, 1st reinforcement fiber layer, middle rubber layer, 2nd reinforcement fibre layer, outer rubber layer: a total of five layers of structure. The dimensions of the submarine hose structure are shown in Table 1.

Table 1. Main structural parameters of submarine hose.

Submarine Hose Structure Parameters	Value	Unit
Inner diameter	500	mm
Thickness of inner rubber layer	8	mm
Thickness of middle rubber layer	14	mm
Thickness of outer rubber layer	7	mm
1st Reinforcement fibre layer	14×1.4	mm
2nd Reinforcement fibre layer	4×1.4	mm
Diameter of steel helix wire	12	mm
Pitch of steel helix wire	50	mm
Winding angle of the fibre layers	45	Deg

The finite element software ABAQUS was applied for parametric modeling. As the layers of the pipe body are tightly bonded and the three rubber layers were constructed as a whole with the same materials, the fiber reinforced layer and the steel helix wire can be separately established, and a reasonable contact relationship with the base rubber be defined. With the purpose of ensuring the accuracy of the model to the greatest extent, the rebar stiffener elements were used as the finite element modeling of the fiber reinforced layer in this paper. Rebar element is suitable for adding reinforcing material to the base element to improve the rigidity of the overall structure. The parameters that need to be defined are rebar element area, element spacing, material properties and included angle. The modeling process of submarine hose structure is shown in the Figure 3.

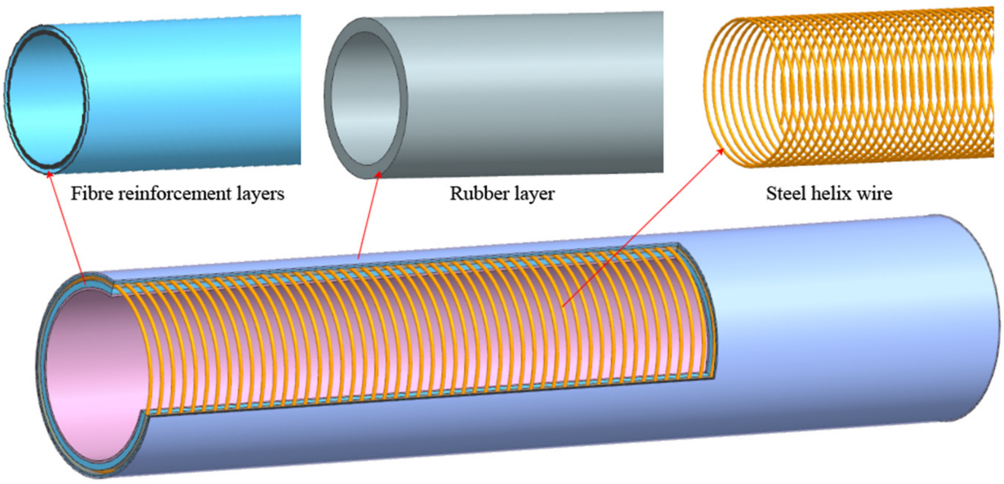

Figure 3. Simple geometric model of submarine hose.

2.2. Material Properties and Constitutive Model

The submarine hose has a complex multilayered reinforced structure. The steel helix wire is an isotropic metal material, and the material parameters are shown in Table 2. In order to simplify the calculation, it is assumed that the fibre reinforced layer is an elastic material.

Table 2. Material properties.

	Elasticity Modulus E (MPa)	Poisson's Ratio	Tensile Strengthσ_u(MPa)	Yield Strength σ_y (MPa)
The steel helix wire	210,000	0.3	1030	645
Fibre reinforcement	1807.35	0.42	_	_

For the hyperelastic material, multiple physical parameters are required to accurately simulate the real deformation law of rubber [23]. Among the multitude of constitutive models of hyperelastic materials, such as the Mooney–Rivilin model, Neo-Hookean model, Yeoh model and Ogden model, the theoretical algorithm of the Ogden model uses the principal stretch instead of the common strain tensor invariant as the reference variable, which can more accurately characterize the mechanical properties of rubber materials. Therefore, the Odgen constitutive model was used in the analysis of rubber tubes in this paper, as shown in Equations (1)–(3), and the material parameters shown in Table 3.

$$W = \sum_{i=1}^{N} \frac{2\mu_i}{\alpha_i} \overline{\lambda}_1^{\alpha_i} + \overline{\lambda}_2^{\alpha_i} + \overline{\lambda}_3^{\alpha_i} - 3 + \sum_{i=1}^{N} \frac{1}{D_i} (J_{el} - 1)^2 \tag{1}$$

$$\overline{\lambda}_i = J^{-\frac{1}{3}} \lambda_i \tag{2}$$

$$J = \lambda_1 \lambda_2 \lambda_3 \tag{3}$$

where N is the order of the model, usually a number between 1–3, μ_i and α_i are the constant of the material. λ_i are the principal stretches, J is the Jacobean determinant, J_{el} is the elastic volume ratio.

Table 3. Material parameters of the rubber.

Material Parameters	Value
μ_1	−1.092
μ_2	0.12
μ_3	4.155
α_1	3.422
α_2	3.993
α_3	−6.601

2.3. Mesh, Loads and Boundary Conditions

The steel helix wire adopts the entity reduced integration C3D8R element, the rubber layer adopts the reduced hybrid C3D8RH element and the cord layer is established by the "Rebar Layer" method and the three-dimensional four-node reduced integration SFM3D4R element is selected [24]. After setting a reasonable grid size, use the structured grid to mesh the submarine hose. The meshing process of submarine hose is shown in Figure 4.

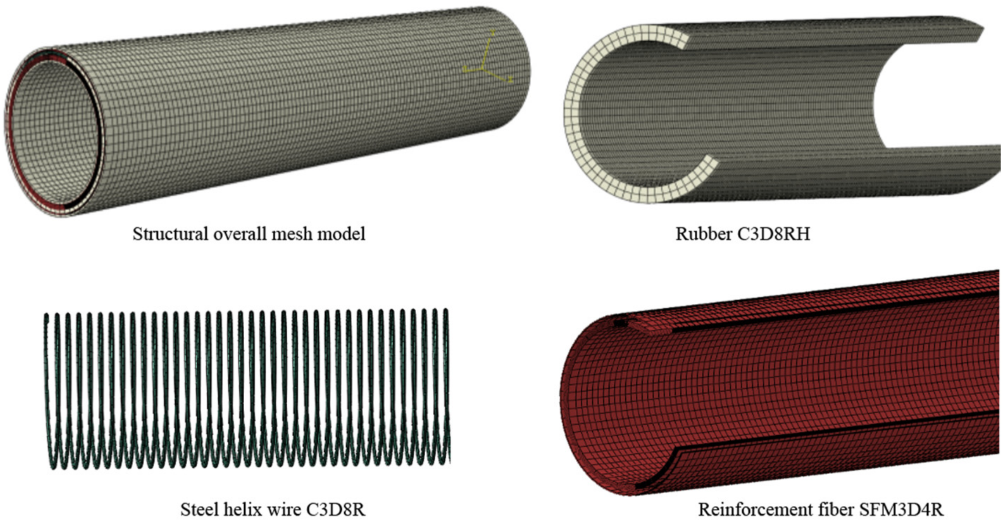

Figure 4. Mesh model of the submarine hose.

It is believed that no relative displacement between the layers of bonded submarine hose. In order to transfer the load completely, the degrees of freedom of each node between the layers are bonded to each other; therefore, the rubber is modeled as a whole in the process of building the model, the steel helix wire and the cord were embedded in the rubber subsequently. Owing to the utilization of the embed technique to achieve the contact relationship, no other inter-layer contact relationships were necessary.

This paper studies the mechanical response of a submarine hose fixed at both ends under uniform external pressure. A relatively long local pipe model was selected considering the possible impact of local effects, and the fixed support was applied at both ends according to the actual situation. The steel helix wire and cord layer have been integrally bound with the rubber tube, which is dispensable to define boundary conditions for them. At the same time, in order to analyze the collapse pressure, a uniform external pressure of 2 MPa is applied to the outer surface of the submarine hose. The interactions, boundary conditions and loading conditions are shown in Figure 5.

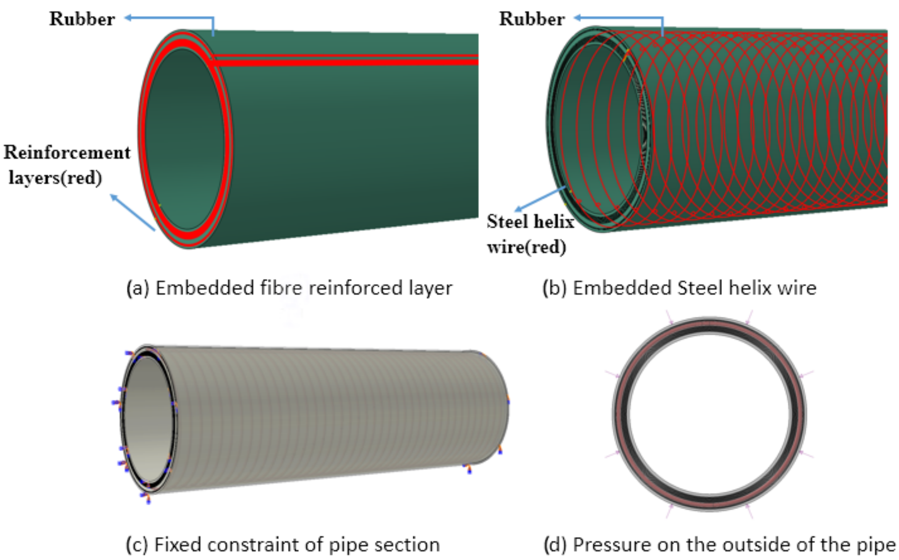

Figure 5. Interaction, loads and boundary conditions: (**a**) Embedded fibre reinforced layer, (**b**) embedded steel helix wire, (**c**) fixed constraint of pipe section, and (**d**) pressure on the outside of the pipe.

3. Results and Discussion

3.1. Finite Element Analysis Results

The hose under the 2 MPa external pressure is calculated by the non-linear Riks method of the ABAQUS software. Figure 6 are the deformed distribution diagrams of the hose. It can be observed that the buckling collapse zone of the hose is close to the middle in the axis direction of the hose. The deformation trend of the hose is similar to the experiment result of the sandwich pipe [19] and SSRTP pipe [20]. The arc length-LPF (Load Proportionality Factor) curve, as shown in Figure 7. The maximum of LPF is 0.625, which indicates that the hose may buckle and collapse when the external pressure is near to 1.25 MPa (0.625 $\times$ 2 MPa). It can be seen that maximum Von Mises stress of the helix wire is 916.4 MPa, which exceeds the yield stress (645 MPa) of the helix wire, shown in Figure 6.

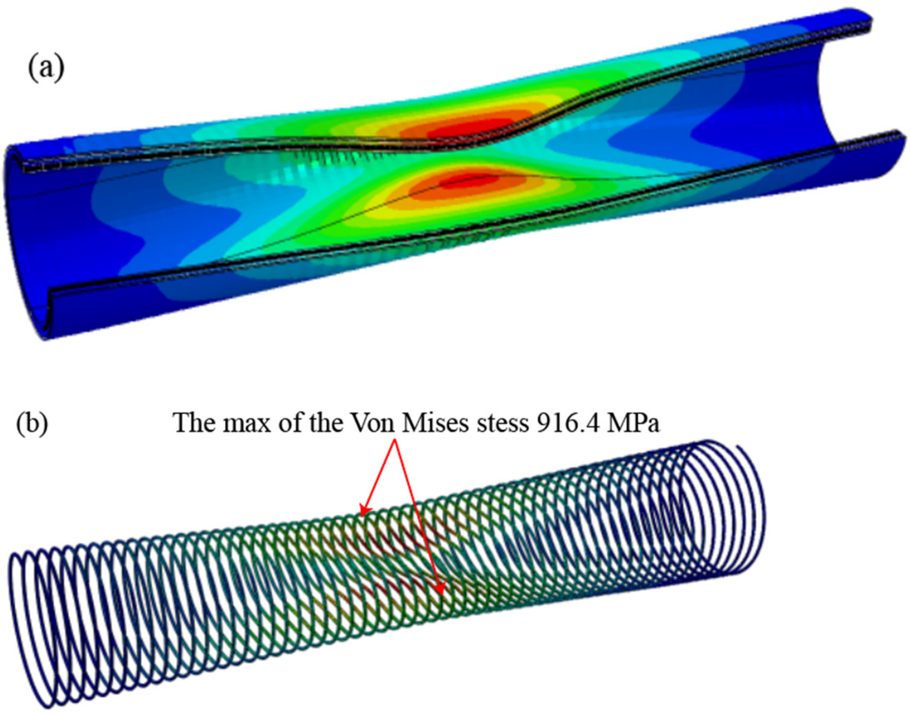

Figure 6. Deformed distribution: (**a**) rubber layers and fiber reinforcement layers; (**b**) steel helix wire.

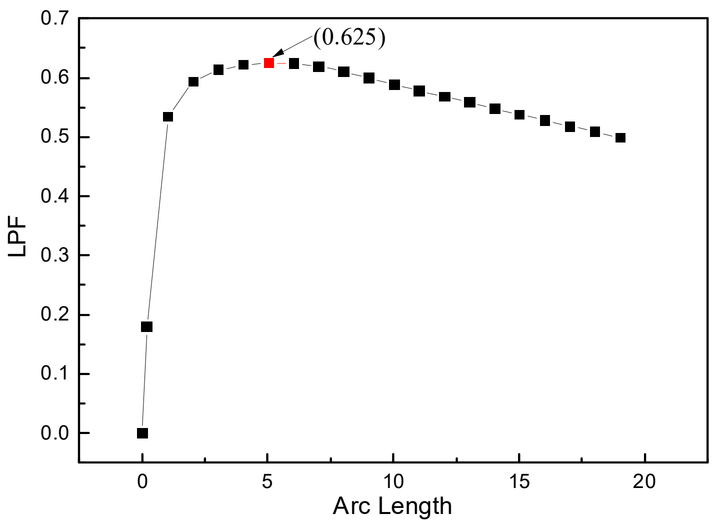

Figure 7. Arc length—LPF curve.

The hose under 1.24 MPa external pressure with non-collapse crush is studied, and the results are shown in Figure 8. The inner and outer cords of the hose have different distribution forms for rebar force (the rebar force is equal to the stress of the fiber reinforcement cord times its cross-sectional area) under the influence of the external pressure of the hose structure. The maximum value of the rebar force on the inner cords (layers 1st~14th) is around 0 degree and 180 degrees at the cross section; it is affected by the ovality of the hose, as shown in Figure 8a,b. However, it is around 240 degrees, and 300 degrees on the outer cords, which is shown in Figure 8c. The maximum of the rebar force on the inner cords is included in the 13th layer. This is because the inner cords close to the helix wire is affected by the helix wire, which causes its maximum of the rebar force to rise quickly, as shown in Figure 8d. The downward general tendency may be seen in the inner cords that separate from the helix wire. Maximum rebar force on the outer cord is rapidly increasing, and the maximum of the rebar force is 12 N, which is located at the 18th layer.

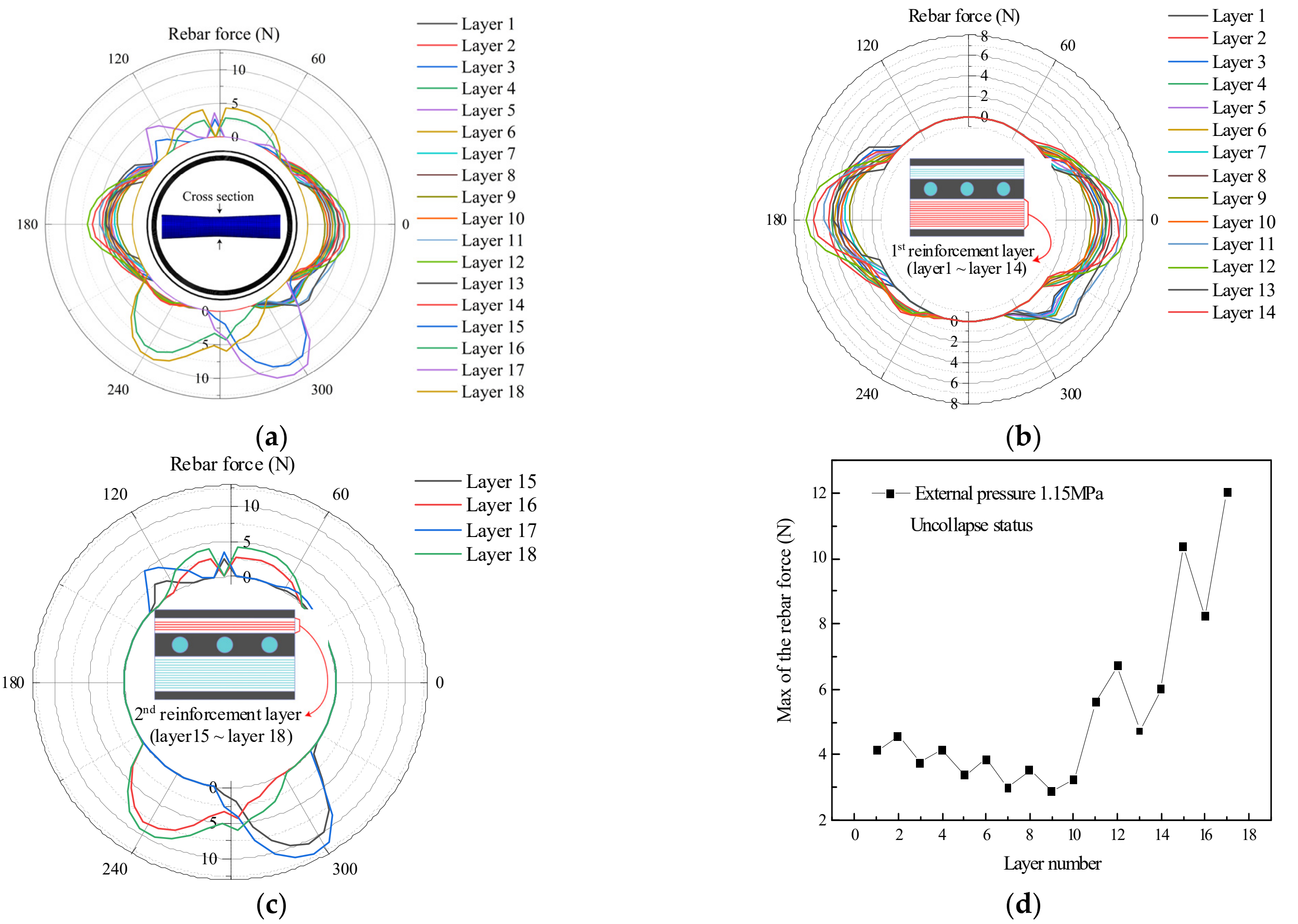

Figure 8. Rebar force of the cord with non-collapse: (**a**) full cords, (**b**) inner cords, (**c**) outer cords, (**d**) maximum of the force in each cord.

When the hose is collapsed at 1 MPa external pressure, the rebar force at the cross section of the hose is shown in Figure 9. Both at around 0 degree and 180 degrees, the rebar force distribution on the cords with non-collapse is comparable to the distribution after collapse. The maximum of the rebar force at the cross section of the hose is 192.59 N, which is located at 18th layer.

The Von Mises stress distribute of the helix wire at the cross section is shown in Figure 10. The Von Mises stress at the cross section is different; the maximum is around 5 degrees and 185 degrees. The maximum of Von Mises stress in the helix wire is 390.67 MPa, when the hose under 1.24 MPa external pressure with non-collapse, as shown in Figure 10a.

The maximums of around 5 degrees, 80 degrees, 185 degrees and 255 degrees; all exceeded the yield strength. The maximum of Von Mises stress in the helix is 765.82 MPa, when the hose collapsed, as shown in Figure 10b. The distribution of Von Mises stress on the helix wire is more greatly different with the rebar force of the cords at the cross section.

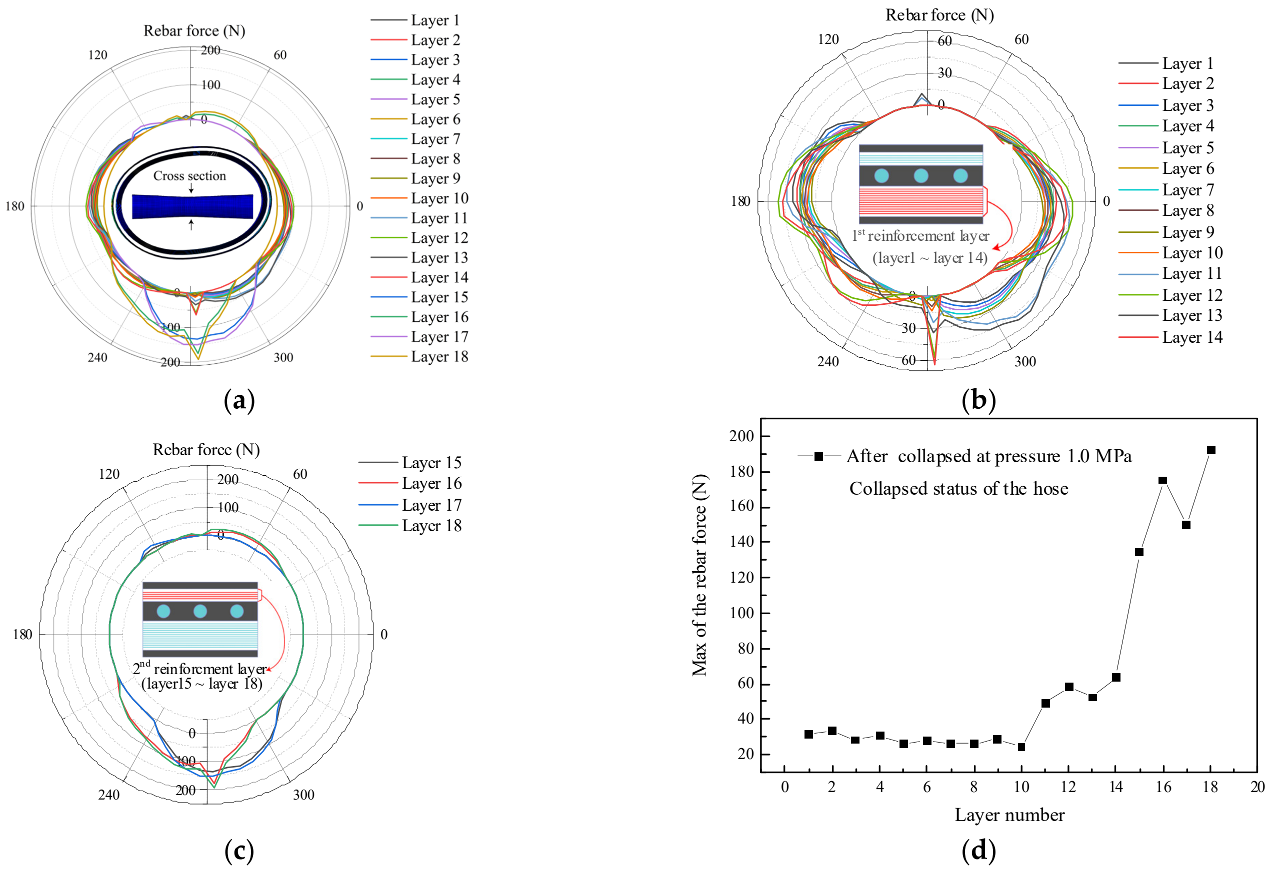

Figure 9. Rebar force of the cord after collapsed: (**a**) full cords, (**b**) inner cords, (**c**) outer cords, (**d**) maximum of the force in each cord.

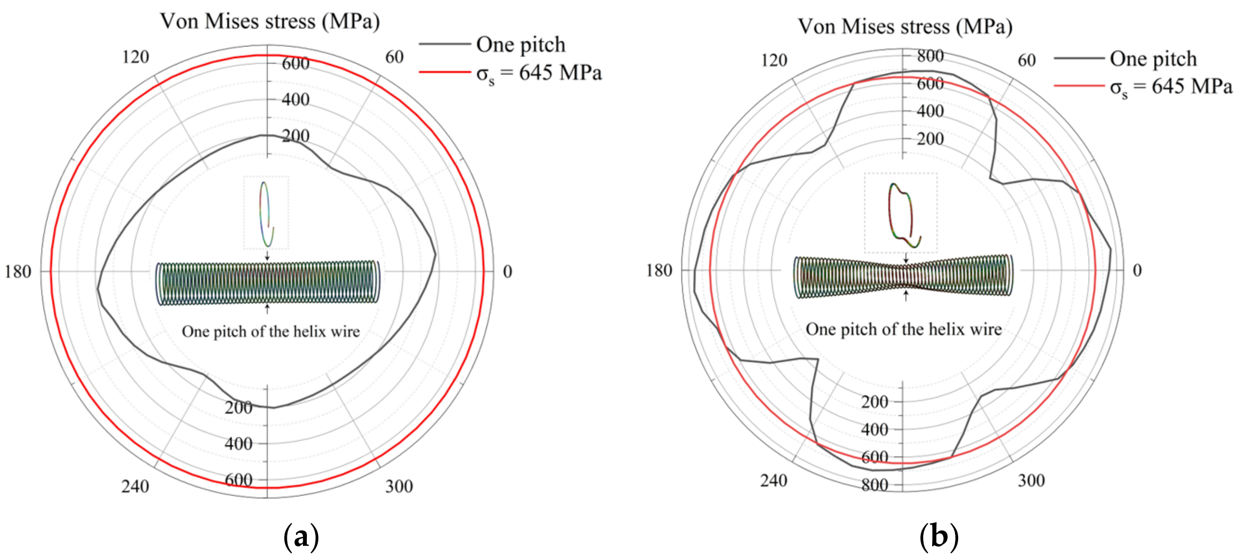

Figure 10. Von Mises stress of the helix wire at cross section of the hose: (**a**) with non-collapse, (**b**) after collapsed.

3.2. Analysis of Initial Ovality

Although the initial ovality of the subsea hoses due to the production process is tiny, the ovality will increase in the process of transportation, installation and laying, thus affecting the crushing performance of the submarine hoses.

It can be seen from Figure 11 that the collapse resistance of the submarine hose is highly influenced by the initial ovality. When the ovality changes from 0.1% to 1%, the ultimate collapse pressure of the submarine hose changes from 1.25 MPa to 1.14 MPa, which is a reduction of 9.12%; obviously, the design of the submarine hose should take into account the initial ovality.

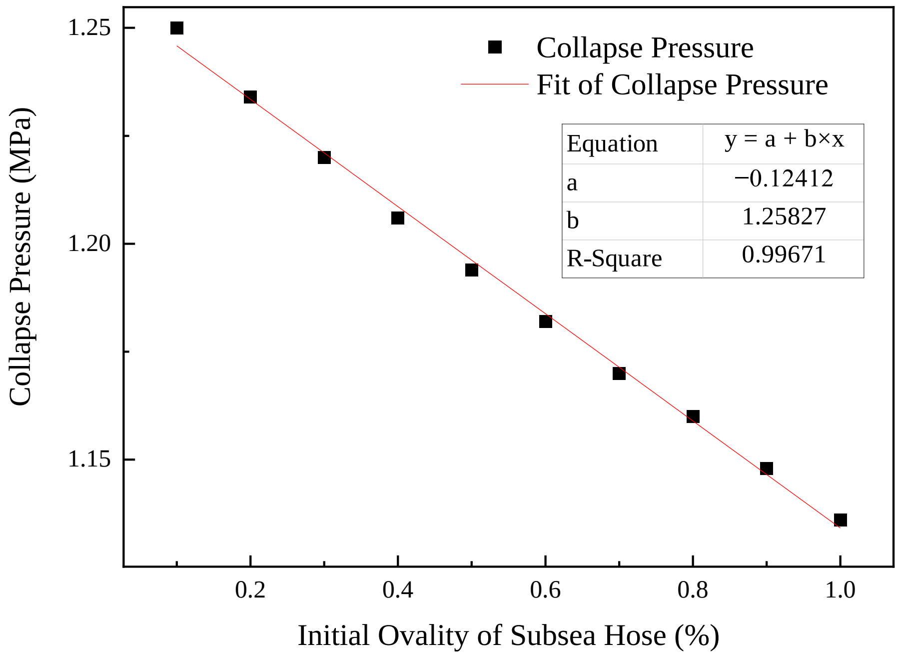

Figure 11. Collapse pressure corresponding to various initial ovality of hose.

3.3. Effect of Helix Wire Material Parameters

According to the analysis in the previous section, the ability of the submarine hose to resist external pressure is mainly provided by the winding steel wire, the material parameter that affects the critical collapse pressure of the submarine hose is mainly the yield stress σ_y of the winding steel wire. In this section, the mechanical response of submarine hoses under uniform external pressure under the yield strength of 12 kinds of spiral wire spiral materials (350~900 MPa) is studied. The initial ovality Δ_0 is 0.5%, and the helix wire diameter d is 12 mm. The pitch of the helix wire is 50 mm, and other material parameters and boundary conditions are the same as before. The collapse bearing capacity obtained by finite element simulation is shown in Figure 12.

It can be clearly seen from Figure 12 that the critical collapse pressure increases with the increase of the yield strength of the steel helix wire. In Figure 13, it can be seen that several response curves begin to diverge with the displacement increasing, which is because the submarine hose begins to yield with the increase of the deformation. It can be clearly seen that by increasing the yield strength of the material, the collapse resistance of the submarine hose can be significantly enhanced.

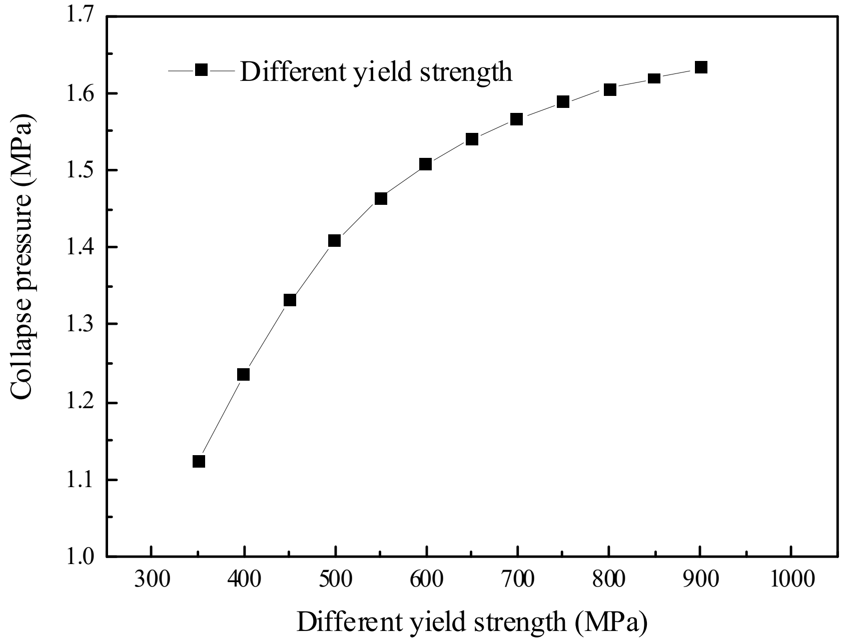

Figure 12. Collapse pressure with different yield strength.

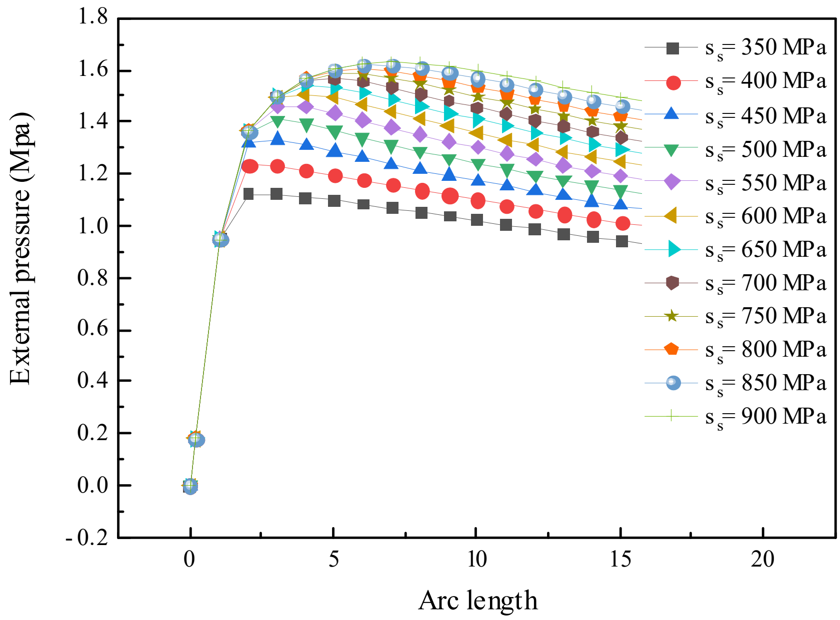

Figure 13. Collapse behavior curve with different yield stress.

Figure 14 shows the variation of the submarine hose collapse pressure with the pitch of the helix wire under different yield strengths of the helix wire. The collapse pressure of the submarine hose with the pitch of 40~60 mm and yield strength of 315 MPa, 645 MPa and 960 MPa were analyzed.

As shown in Figure 14, the yield strength of submarine hose is influenced by the yield strength of steel helix wire. The collapse pressure of the submarine hose increases with the increase of the yield strength, while the greater the pitch of the helix wire, the smaller the influence of the helix wire yield strength is, and vice versa.

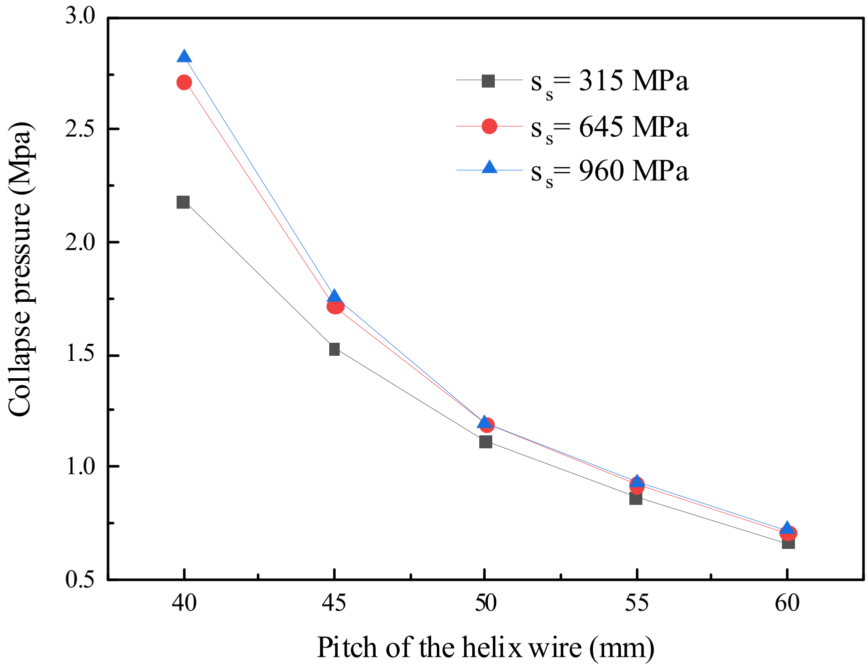

Figure 14. Pressure capacity vs. pitches of helix wire for submarine hose with different yield strength.

3.4. Effect of the Influence for Winding Steel Wire Geometrical Parameters

3.4.1. Effect of Helix Wire Diameter

This section studies the mechanical response of submarine hoses with six helix wire diameters (10 mm, 11 mm, 12 mm, 13 mm, 14 mm and 15 mm) under uniform external pressure. The initial ovality Δ_0 of the submarine hose is 0.5%, the spiral pitch s of the winding steel wire is 50 mm, and other material parameters and boundary conditions are identical to the previous parameters. The collapsed bearing capacity is obtained by finite element simulation, which is shown in Figure 15.

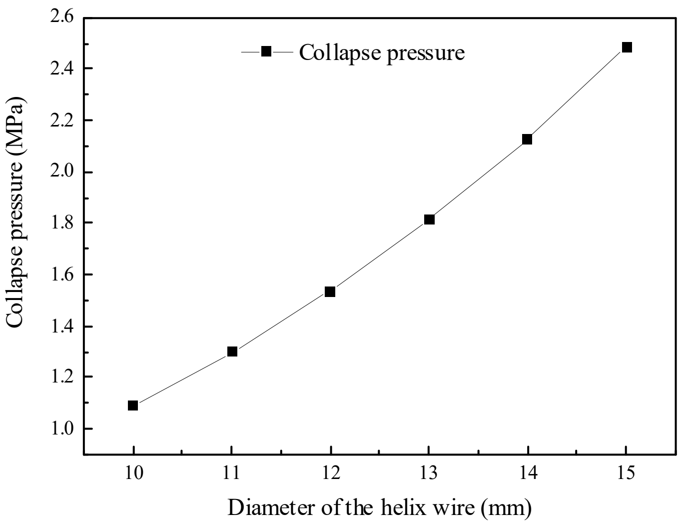

Figure 15. Collapse pressure of submarine hose corresponding to different helix wire diameters.

It can be seen from Figure 15 that increasing the diameter of the steel helix wire is of great help for improving the compressive performance of the submarine hose. When the diameter of the steel helix wire changes within 10~15 mm, the ultimate collapse pressure of the submarine hose rises from 1.09 MPa to 2.48 MPa, increasing by 128.3%. Therefore, the influence of the diameter of the steel helix wire has to be considered in the collapse design of the submarine hose.

Figure 16 shows the buckling behavior curve of submarine hoses under uniform external pressure with different helix wire diameters.

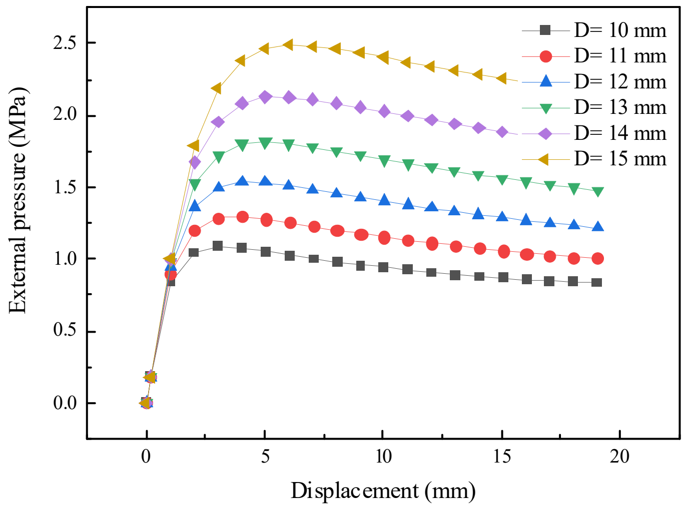

Figure 16. Collapse behavior curve for submarine hose with various helix wire diameters.

It can be seen from Figure 16 that the displacement load curve of the hose considering the initial ovality slowly drops after a period of rise and then tends to be stable; the load value at the inflection point is the critical collapse pressure of the submarine hose model. In accordance with Figure 15, critical collapse pressure increased with the increase of helix wire diameter increasing. It can also be seen from Figure 16 that the displacement–load curve rises as the diameter of the helix wire increases, which means that in order to obtain the same radial displacement, smaller external pressure needs to be applied when the diameter of the helix wire is smaller. Under the same external pressure, the larger the diameter of the helix wire, the smaller the radial displacement.

3.4.2. Effect of Helix Wire Pitch

This section studied the mechanical response of submarine hoses with five helix wire pitches (40 mm, 45 mm, 50 mm, 55 mm and 60 mm) under uniform external pressure. The initial ovality Δ_0 is 0.5%, and the helix wire diameter d is 12 mm, the same conditions and other parameters were applied as before. The collapse pressure with different helix wire pitches is shown in Figure 17.

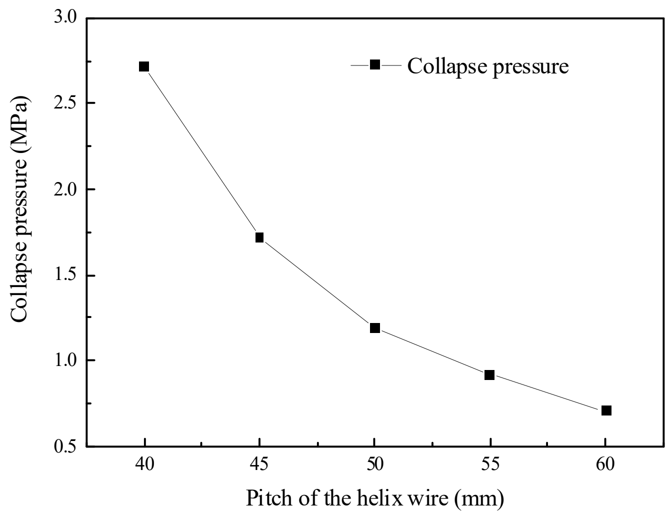

Figure 17. Collapse pressure of submarine hose corresponding to various pitches of helix wire.

It can be seen from Figure 17 that the helix wire pitch has a great impact on the collapse pressure of the submarine hose. When the pitch of the helix wire changes from 40 mm to 60 mm, the ultimate collapse pressure of the submarine hose changes from 2.71 MPa dropped to 0.71 MPa, a decrease of 64%. It can be seen that the influence of the helix wire pitch on the collapse bearing capacity cannot be ignored. It can also be seen that as the pitch of the helix wire increases, the influence of the pitch on the collapse pressure of the submarine hose will decrease.

3.4.3. Comprehensive Influence Analysis of Helix wire Diameter and Pitch

Figure 18 shows the corresponding relationship between the collapse pressure of the submarine hose and the diameter of the helix wire under different helix wire pitches. The collapse pressure of submarine hoses with helix wire pitch between 40 and 60 mm and helix wire diameter between 10 mm and 15 mm is analyzed.

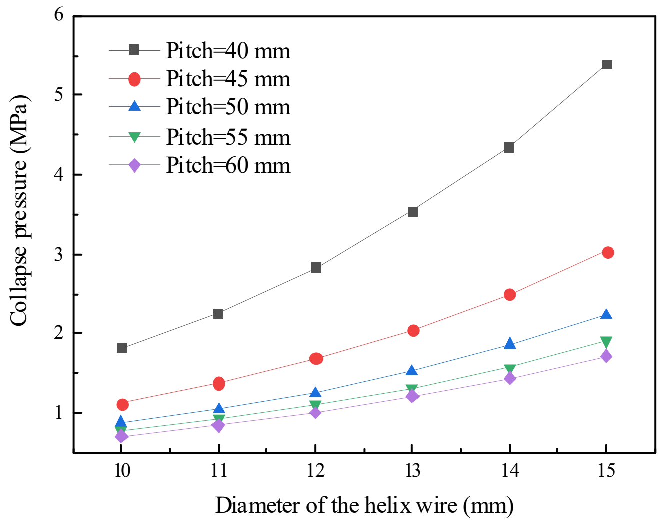

Figure 18. Collapse pressure vs. helix wire diameters in different pitch of the helix wire.

Figure 18 combines the influence of the diameter and pitch of the helix wire on the collapse pressure of the submarine hose. It can be seen that as the pitch of the helix wire increases, the diameter of the helix wire has an effect on the collapse pressure of the submarine hose. When the helix wire pitch is 40 mm, the diameter increases from 10 mm to 15 mm, and the collapse pressure of the submarine hose increases by 197%. When the helix wire pitch is 60 mm, the diameter increases from 10 mm to 15 mm. The collapse pressure of the submarine hose has increased by 142%. Although the influence of the diameter of the steel wire is reduced, the collapse pressure of the submarine hose by the diameter of the winding steel wire is still very large. At the same time, it can be seen that when the pitch of the winding steel wire is greater than 50 mm, the pitch has less influence on the collapse pressure of the submarine hose. Therefore, the impact of the diameter of the helix wire on the performance should be fully considered.

4. Theoretical Research on Collapse Pressure of Submarine Hose

4.1. The Prediction Formula of Collapse Pressure

At present, there is no suitable prediction formula for the calculation of the collapse pressure of submarine hoses. In this paper, 164 sets of finite element models of submarine hoses with different parameter combinations are obtained through parametric modeling, and the corresponding collapse pressure is obtained. Comprehensive effect of diverse parameters including the initial ovality, the diameter of the helix wire, the pitch of the helix wire and the yield strength of the helix wire material on the collapse pressure of the submarine hose are considered. Based on the numerical results of these models, it can be used to perform nonlinear fitting to obtain the prediction formula of the collapse pressure of submarine hose [20].

Based on the analysis in the previous section, the collapse pressure can be expressed as:

$$P_{cr} = f(\Delta_0,\ \mathrm{d},\ \mathrm{s},\ \mathrm{D}, \sigma_y, \mathrm{E}, \nu) \tag{4}$$

P_{cr} represents the collapse pressure of the submarine hose, Δ_0 is the initial ovality of the submarine hose, d is the diameter of the helix wire, s is the pitch of the helix wire, D is the diameter of the helix wire, σ_y is the yield strength of the helix wire material, E is the elastic modulus of the helix wire and ν is the Poisson's ratio of the helix wire. The value of Poisson's ratio ν is generally taken as 0.3. In order to improve the calculation efficiency, the dimensionless Formula (4) can be expressed as:

$$\frac{P_{cr}}{\sigma_y} = f\left(\frac{d}{s}, \frac{d}{D}, \frac{\sigma_y}{\mathrm{E}}, \Delta_0\right) \tag{5}$$

Based on Formula (5), combined with the numerical results obtained by parametric modeling, the prediction formula for the collapse pressure of the submarine hose can be expressed as:

$$\begin{aligned}\frac{P_{cr}}{\sigma_y} = a_1\left(\frac{d}{s}\right)^{a_2} & \left(\frac{d}{D}\right)^{a_3}(\Delta_0)^{a_4} + a_5\left(\frac{d}{s}\right)^{a_6}\left(\frac{d}{D}\right)^{a_7}\left(\frac{\sigma_y}{\mathrm{E}}\right)^{a_8} \\ & + a_9\left(\frac{d}{s}\right)^{a_{10}}\left(\frac{d}{D}\right)^{a_{11}}\left(\frac{\sigma_y}{\mathrm{E}}\right)^{a_{12}}(\Delta_0)^{a_{13}}\end{aligned} \tag{6}$$

Nonlinear least squares method is used to perform nonlinear fitting on the obtained results, and the values of a_1~a_{13} are shown in Table 4.

Table 4. Unknown parameter values obtained by fitting.

Parameter	Value
a_1	1.594×10^{-7}
a_2	7.330
a_3	−4.473
a_4	0.003
a_5	8.004×10^{-4}
a_6	−1.248
a_7	1.709
a_8	−0.749
a_9	2.181×10^{-5}
a_{10}	4.211
a_{11}	−0.441
a_{12}	−1.091
a_{13}	−0.180

The prediction formula is:

$$\begin{aligned}\frac{P_{cr}}{\sigma_y} = 1.594e^{-7}\left(\frac{d}{s}\right)^{7.330} & \left(\frac{d}{D}\right)^{-4.473}(\Delta_0)^{0.003} + 8.004e^{-4}\left(\frac{d}{s}\right)^{-1.248}\left(\frac{d}{D}\right)^{1.709}\left(\frac{\sigma_y}{\mathrm{E}}\right)^{-0.749} \\ & + 2.181e^{-5}\left(\frac{d}{s}\right)^{4.211}\left(\frac{d}{D}\right)^{-0.441}\left(\frac{\sigma_y}{\mathrm{E}}\right)^{-1.091}(\Delta_0)^{-0.180}\end{aligned} \tag{7}$$

4.2. Comparison of Finite Element Results and Formula Results

According to the obtained prediction formula, Table 5 lists some relevant parameters and the results of finite element simulation and prediction formula, and calculates the error value of the prediction formula. The error value result shows that the prediction formula value is in good agreement with the finite element result. Through calculation, the average error value between prediction formula and finite element simulation results is 1.792%, the maximum of 9.4823% and the minimum error value of 0.0322% are determined, respectively, which is within the acceptable range.

Table 5. FEM results compared with predictions from Equation (7).

Δ_0	*d* (mm)	*D* (mm)	*s* (mm)	E (MPa)	σ_y (MPa)	P_{cr}-FE (MPa)	P_{cr} Fit (MPa)	Error
0.10%	12	592.4	50	210,000	645	1.376	1.425	3.55%
0.20%	12	592.4	50	210,000	645	1.337	1.345	0.61%
0.30%	12	592.4	50	210,000	645	1.307	1.303	−0.27%
0.40%	12	592.4	50	210,000	645	1.291	1.275	−1.19%
0.50%	12	592.4	50	210,000	645	1.250	1.255	0.34%
0.60%	12	592.4	50	210,000	645	1.241	1.238	−0.21%
0.70%	12	592.4	50	210,000	645	1.219	1.225	0.51%
0.80%	12	592.4	50	210,000	645	1.199	1.214	1.19%
0.90%	12	592.4	50	210,000	645	1.175	1.204	2.51%
1.00%	12	592.4	50	210,000	645	1.162	1.195	2.90%
0.50%	10	590.4	50	210,000	315	0.766	0.752	−1.87%
0.50%	11	591.4	50	210,000	315	0.911	0.906	−0.59%
0.50%	12	592.4	50	210,000	315	1.086	1.097	0.98%
0.50%	13	593.4	50	210,000	315	1.313	1.330	1.30%
0.50%	14	594.4	50	210,000	315	1.580	1.613	2.07%
0.50%	15	594.4	50	210,000	315	1.886	1.951	3.46%
0.50%	12	592.4	40	210,000	960	2.975	3.238	8.85%
0.50%	12	592.4	45	210,000	960	1.770	1.937	9.48%
0.50%	12	592.4	50	210,000	960	1.331	1.392	4.58%
0.50%	12	592.4	55	210,000	960	1.163	1.156	−0.58%
0.50%	12	592.4	60	210,000	960	1.064	1.064	0.03%

Figures 19–22 show the comparison curves of some finite element results and the results of the prediction formula, respectively, showing the finite element values and predictions of the helix wires of different materials with different initial ovality, different helix wire diameters and helix wire pitches. The comparison shows that the finite element value and the predicted formula value are in good agreement with each other.

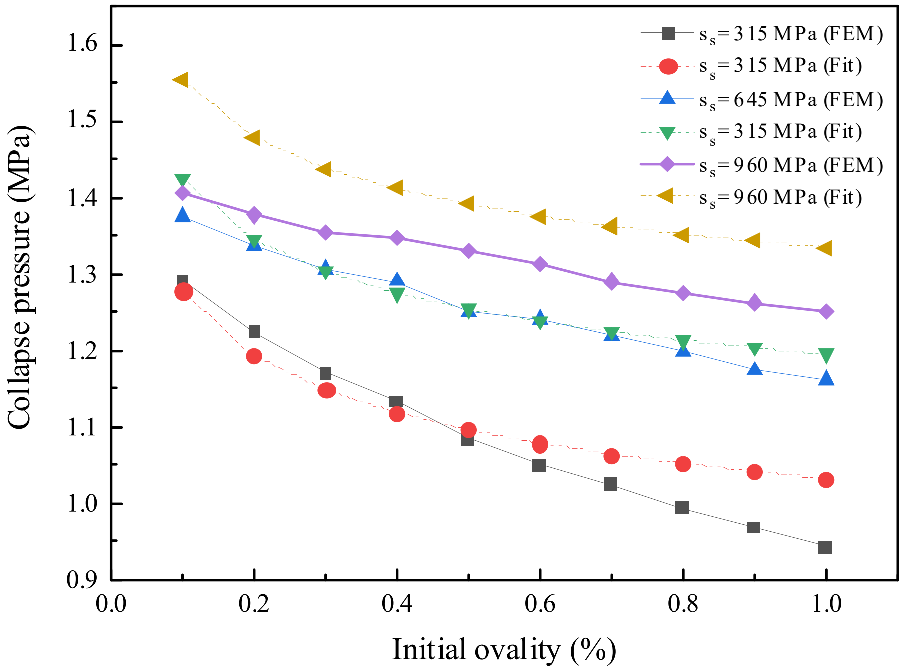

Figure 19. Comparison of FEM and fitting results with respect to different initial ovality.

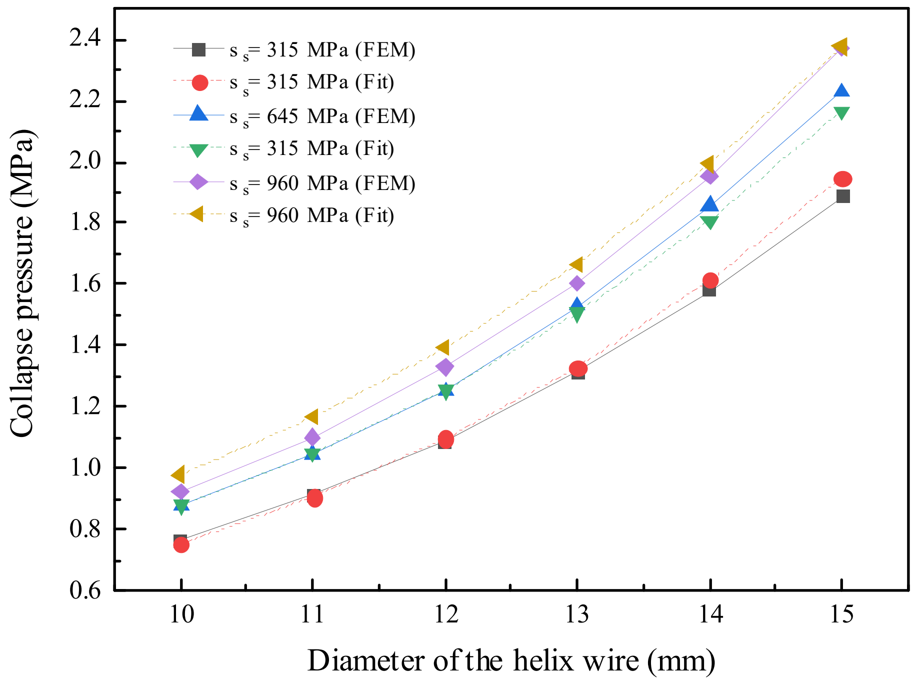

Figure 20. Comparison of FEM and fitting results with respect to different helix wire diameters.

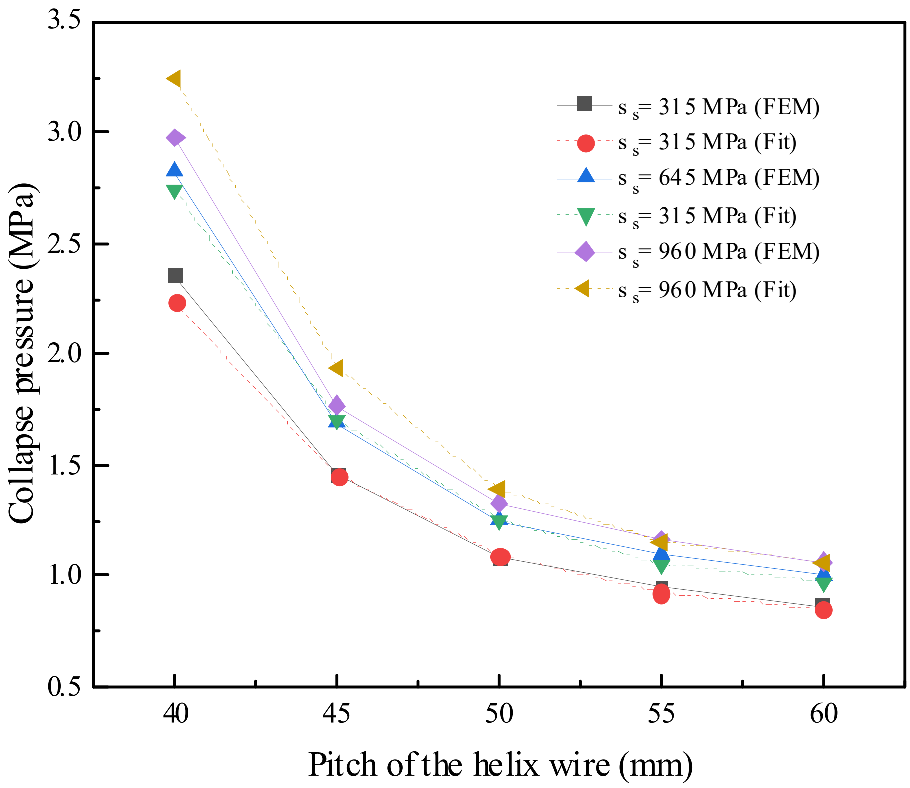

Figure 21. Comparison of FEM and equation results with respect to different distances of helix wire.

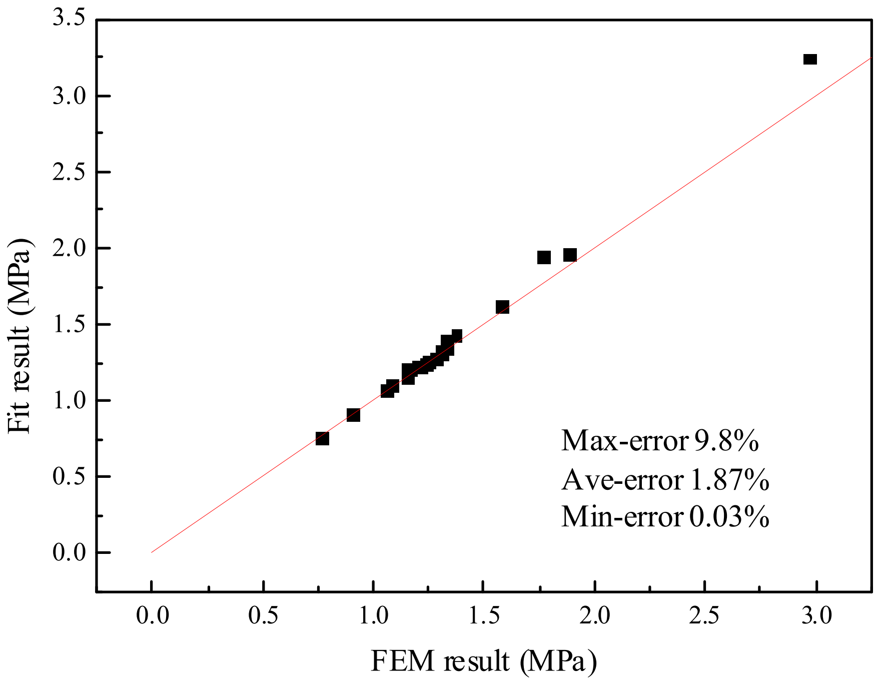

Figure 22. Correlation results between the prediction formula and the finite element model.

5. Conclusions

A continuous increase in global demand for oil and gas has promoted the development of offshore oil and promoted the development of the submarine hose. This work studies the influence of winding steel wire on the collapse bearing capacity of submarine hoses. The main conclusions are listed as follows:

(1) The finite element model of the submarine hose was established, and the collapse pressure of the submarine hose under uniform distribution pressure was analyzed. The collapse pressure of the submarine hose was obtained and the structure of each layer was analyzed. It is concluded that the winding steel wire layer is the main structure of the submarine hose to resist uniform external pressure. As the submarine hose reaches the collapse pressure, the stress of the winding steel wire also reaches the yield strength simultaneously; the deformation is known as plastic deformation.

(2) In order to further study the influence of the geometric parameters and material parameters of the helix wire on the collapse pressure of the submarine hose, the initial ovality, the diameter of the helix wire, the pitch of the helix wire and the yield strength of the steel wire are combinatorial analyzed for different submarine hoses. Using Python language for parametric modeling, numerous submarine hose models are obtained, and ABAQUS collapse analysis is performed to obtain the corresponding collapse pressure.

(3) According to the large number of finite element values obtained, considering the effect of each parameter, the analysis shows that the greater the initial ovality of submarine hose, the smaller the collapse pressure; the larger the diameter of the helix wire, the greater the collapse pressure of the submarine hose; the greater the spiral pitch of the helix wire, the lower the collapse pressure of the submarine hose; but as the pitch of the spiral helix wire increases, the influence of the pitch on the collapse pressure of the submarine hose decreases accordingly; the greater the yield strength of the steel wire, the greater the collapse pressure of the submarine hose. As the yield strength increases, the influence of the yield strength on the collapse pressure of the submarine hose will be reduced.

(4) For the submarine hose with initial ovality, based on a large number of finite element simulation results, the numerical analysis is used to obtain the prediction formula of the collapse pressure of the submarine hose. Then the formula value is compared with the finite element result. When the error value between the prediction formula value and the finite element analysis result is within 10%, the prediction formula is considered to be

reasonable to predict the collapse pressure of submarine hoses. Further studies using the neural network model combing with a larger numbers of 3D finite element results may be performed in the follow-up study for the optimal solution of the limit states analysis of the marine hose.

Author Contributions: Conceptualization, D.W. and Y.H.; methodology, D.W.; software, D.W.; validation, D.W., J.Z. and C.G.; formal analysis, J.Z.; investigation, J.Z. and Y.H.; resources, C.A.; data curation, C.G; writing—original draft preparation, C.G.; writing—review and editing, D.W. and C.A.; visualization, D.W.; supervision, C.A.; project administration, C.A.; funding acquisition, C.A. and J.Z. All authors have read and agreed to the published version of the manuscript.

Funding: This research was funded by the National Natural Science Foundation of China (Grant no. 51879271), the Project of Ministry of Industry and Information Technology of the People's Republic of China (Research on the Key Technology of Treatment Process for High-flow Offshore Natural Gas, CJ09N20).

Institutional Review Board Statement: Not applicable.

Informed Consent Statement: Not applicable.

Data Availability Statement: Not applicable.

Acknowledgments: The authors would like to thank reviewers for their useful and helpful comments on the manuscript.

Conflicts of Interest: The authors declare no conflict of interest.

References

1. Flory, J.F.; Mascenik, J.F.; Pedersen, K.I. The single anchor leg mooring. In Proceedings of the Offshore Technology Conference, Houston, TX, USA, 30 April 1972.
2. Amaechi, C.V.; Wang, F.; Ye, J. Mathematical modelling of bonded marine hoses for single point mooring (SPM) systems, with Catenary Anchor Leg Mooring (CALM) buoy application—A review. *J. Mar. Sci. Eng.* **2021**, *9*, 1179. [CrossRef]
3. Wei, D.; An, C.; Zhang, Z.; Zhang, J.; Zhang, A.X. Collapse Response of a single carcass offshore rubber hose under bending moment (ISOPE-I-22-175). In Proceedings of the 32nd International Ocean and Polar Engineering Conference, Shanghai, China, 5 June 2022.
4. Pecher, A.; Foglia, A.; Kofoed, J.P. Comparison and sensitivity investigations of a CALM and SALM type mooring system for wave energy converters. *J. Mar. Sci. Eng.* **2014**, *2*, 93–122. [CrossRef]
5. Deng, Y. Damage Research and Extreme Response of Submarine Hose Subjected to Wave Loads at Maoming Single Point Mooring. Master's Thesis, South China University of Technology, Guangzhou, China, 2011.
6. Oil Companies International Marine Forum. *Guide to Purchasing and Manufacturing Hoses for Offshore Moorings*, 5th ed.; Oil Companies International Marine Forum: London, UK, 2009.
7. American Petroleum Institute. *API Spec 17: Specification for Bonded Flexible Pipe*, 3rd ed.; American Petroleum Institute: Washington, DC, USA, 2017.
8. Amaechi, C.V.; Chesterton, C.; Butler, H.O.; Gu, Z.W. Numerical modelling on the local design of a Marine Bonded Composite Hose (MBCH) and its helix reinforcement. *J. Compos. Sci.* **2022**, *6*, 79. [CrossRef]
9. Gao, Q.; Zhang, P.; Duan, M.L.; Yang, X.Q.; Shi, W.B.; An, C.; Li, Z.L. Investigation on structural behavior of ring-stiffened composite offshore rubber hose under internal pressure. *Appl. Ocean Res.* **2018**, *79*, 7–19. [CrossRef]
10. Tonatto, M.L.; Tita, V.; Araujo, R.T.; Forte, M.M.; Amico, S.C. Parametric analysis of an offloading hose under internal pressure via computational modeling. *Mar. Struct.* **2017**, *51*, 174–187. [CrossRef]
11. Shahzamanian, M.M.; Kainat, M.; Yoosef-Ghodsi, N.; Adeeb, S. Systematic literature review of the application of extended finite element method in failure prediction of pipelines. *J. Pipeline Sci. Eng.* **2021**, *1*, 241–251. [CrossRef]
12. Elyasi, N.; Shahzamanian, M.; Lin, M.; Westover, L.; Li, Y.; Kainat, M.; Yoosef-Ghodsi, N.; Adeeb, S. Prediction of Tensile Strain Capacity for X52 Steel Pipeline Materials Using the Extended Finite Element Method. *Appl. Mech.* **2021**, *2*, 209–225. [CrossRef]
13. Huang, T.S.; Leonard, J.W. Lateral stability of a submarine flexible hoseline. *Ocean Eng.* **1990**, *17*, 35–52. [CrossRef]
14. Ma, J.; Yang, Z.; Liang, Y.T.; Xu, N.; Zhang, H.R.; Huang, Z.L. Numerical simulation of submarine hoses for catenary single point mooring system. *China PET Mach.* **2017**, *45*, 39–44.
15. Yang, W.; Zhang, Y.H.; Sun, G.M. Design research of submarine hose with Chinese lantern configuration used in CALM system. *Ocean Eng. Equip. Technol.* **2018**, *5*, 165–173.
16. Wang, F.; Amaechi, C.V.; Hou, X.N.; Ye, J.Q. Sensitivity studies on offshore submarine hoses on CALM buoy with comparisons for Chinese-Lantern and Lazy-S configuration (OMAE2019-96755). In Proceedings of the 38th International Conference on Ocean, Offshore and Arctic Engineering ASME OMAE, Glasgow, UK, 30 August 2019.

17. Amaechi, C.V.; Wang, F.; Hou, X.N.; Ye, J.Q. Strength of submarine hoses in Chinese-lantern configuration from hydrodynamic loads on CALM buoy. *Ocean Eng.* **2019**, *171*, 429–442. [CrossRef]
18. Wei, D.; An, C.; Wu, C.; Duan, M.L.; Estefenet, S.F. Torsional structural behavior of composite rubber hose for offshore applications. *Appl Ocean Res.* **2022**, *128*, 103333. [CrossRef]
19. An, C.; Duan, M.; Filho, R.D.T.; Estefen, S.F. Collapse of sandwich pipes with PVA fiber reinforced cementitious composites core under external pressure. *Ocean Eng.* **2014**, *82*, 1–13. [CrossRef]
20. Bai, Y.; Liu, T.; Cheng, P.; Yuan, S.; Yao, D.; Tang, G. Buckling stability of steel strip reinforced thermoplastic pipe subjected to external pressure. *Compos. Struct.* **2016**, *152*, 528–537. [CrossRef]
21. Bai, Y.; Han, P.; Liu, T.; Yuan, S.; Tang, G. Mechanical responses of metallic strip flexible pipe subjected to combined bending and external pressure. *Ships Offshore Struct.* **2018**, *13*, 320–329. [CrossRef]
22. Yang, J.; Paz, C.M.; Estefen, S.F.; Fu, G.; Lourenco, M.I. Collapse pressure of sandwich pipes with strain-hardening cementitious composite-part 1: Experiments and parametric study. *Thin-Walled Struct.* **2020**, *148*, 106605. [CrossRef]
23. Austrell, P.E.; Olsson, A.K. Modelling procedures and properties of rubber in rolling contact. *Polym. Test.* **2013**, *32*, 306–312. [CrossRef]
24. He, T.T.; Duan, M.L.; Wang, J.L.; Lv, S.S.; An, C. On the external pressure capacity of deepwater sandwich pipes with inter-layer adhesion conditions. *Appl. Ocean Res.* **2015**, *52*, 115–124. [CrossRef]